Metal Free-Covalent Triazine Frameworks as Oxygen Reduction Reaction Catalysts – Structure-Electrochemical Activity Relationship

Turgut Sönmez,‡[a,b] Kendra Solveig Belthle,‡[a,c] Andree Iemhoff,[a] Jan Uecker,[a] Jens Artz,[a] Timo Bißwanger,[d] Christoph Stampfer,[d] Hairul Hisham Hamzah,[e] Sabina Alexandra Nicolae,[f] Maria-Magdalena Titirici[f] and Regina Palkovits*[a]

[a.] Institut für Technische und Makromolekulare Chemie RWTH Aachen University, Worringerweg 2, 52074 Aachen, Germany

[b.] Department of Energy Systems Engineering, Technology Faculty, Karabük University, 78050 Karabük, Turkey

[c.] Max-Planck-Institut für Kohlenforschung, Kaiser-Wilhelm-Platz 1, Mülheim an der Ruhr, D-45470, Germany

[d.] JARA-FIT and 2nd Institute of Physics A, RWTH Aachen University, 52074 Aachen, Germany

[e.] School of Chemical Sciences, Universiti Sains Malaysia (USM), 11800, Gelugor, Penang, Malaysia

[f.] School of Engineering and Materials Science and Materials Research Institute, Queen Mary University of London, London E14 NS, UK

‡ These authors contributed equally to this work

*Corresponding Author
E-mail: palkovits@itmc.rwth-aachen.de

Table S1. *Elemental analysis of all CTF materials used in this study*

CTF	C [wt.%]	H [wt.%]	N [wt.%]
DCP	60.21	3.233	18.84
*p*DCB	78.23	2.291	11.38
DCBP	84.96	1.872	5.31
*p*DCB-400	72.66	3.587	13.47
*p*DCB-600	78.23	2.291	11.38
*p*DCB-750	76.10	1.565	6.25
DCBP-750	87.15	1.245	3.36

Table S2. *Theoretical nitrogen contents and C/N molar ratios for each monomer used for all synthesized CTF materials.*

CTF	Monomer	N [wt.%]	C/N
DCP	2,6-dicyanopyridine	32.5	2.3
*p*DCB	1,4-dicyanobenzene	21.9	4.0
DCBP	4,4'-biphenyldicarbonitrile	13.7	7.0
*p*DCB-400	1,4-dicyanobenzene	21.9	4.0
*p*DCB-600	1,4-dicyanobenzene	21.9	4.0
*p*DCB-750	1,4-dicyanobenzene	21.9	4.0
DCBP-750	4,4'-biphenyldicarbonitrile	13.7	7.0

Table S3. *Chemical composition of all CTF materials in this study obtained by X-ray photoelectron spectroscopy (XPS)*

CTF	**Atomic %**									
	C1s	N1s	O1s	Co2p	Cu2p	Cl2p	Rh3d	Na1s	Zn2p	Si2p
DCP	74.72	18.31	5.54	-	-	-	-	1.49	0.43	0.51
*p*DCB	83.38	8.94	4.07	-	-	0.29	-	0.29	-	-
DCBP	91.25	3.77	4.58	-	-	0.41	-	-	-	-
*p*DCB-400	83.64	11.05	4.36	-	-	-	-	0.94	-	-
*p*DCB-600	83.38	8.94	4.07	-	-	0.29	-	0.29	-	-
*p*DCB-750	90.77	5.55	3.21	-	-	-	0.47	-	-	-
DCBP-750	93.62	2.06	4.32	-	-	-	-	-	-	-

Table S4. *Rct values, fitting errors, convergence fit values, convergence and proposed circuit obtained from fitted EIS for each CTF material based on the proposed equivalent circuits as shown in Figure S8A, S8B and S8C.*

CTF	*R*ct [ohm]	Fitting error [%]	Convergence fit [x^2]	Convergence	Proposed Circuit
DCP	48.75	9.86	0.432	yes	Figure S8A
*p*DCB	270.18	27.14	3.097	yes	Figure S8A
DCBP	165.73	154.09	2.730	yes	Figure S8B
*p*DCB-400	752.49	25.74	2.640	yes	Figure S8A
*p*DCB-600	270.18	27.14	3.097	yes	Figure S8A
*p*DCB-750	41.55	12.59	0.7142	yes	Figure S8A
DCBP-750	2253	3.136	0.191	yes	Figure S8C

Table S5. *Comparison of the reported CTF materials with other state of the art metal-free carbon based catalysts in terms of onset potential, half-wave potential and limiting current density in alkaline media.*

Catalysts	E_o [V *vs.* RHE]	$E_{1/2}$ [V *vs.* RHE]	$J_{m\ (@\sim 0.2\ V\ vs.\ RHE)}$ [mA cm^{-2}]	Electrolyte	Rotation Speed (rpm)	Mass Loading (g cm^{-2})	Reference
*p*DCB	0.84	0.68	-6.6	0.1 M KOH	2500	0.20	This study
DCBP-750	**0.90**	**0.79**	**-5.1**	**0.1 M KOH**	**2500**	**0.20**	**This study**
10% wt. Pt/C	0.96	0.82	-6.9	0.1 M KOH	2500	0.20	This study
CTF-Super P-10	0.98	0.88	-5.3	0.1 M KOH	1600	0.70	1
CTF	1.01	0.88	-4.76	0.1 M KOH	1600	0.70	1
N-Graphene	0.77	0.67	-0.87	0.1 M KOH	2000	0.04	2
NC	0.73	0.66	-2.7	0.1 M KOH	1600	0.21	3
NG-900-1	0.82	0.66	-4.4	0.1 M KOH	2500	0.50	4
NG-900-4	0.84	0.77	-4.8	0.1 M KOH	2500	0.50	4
CTF-CSU1	0.79	0.57	-4.9	0.1 MKOH	1600	0.20	5
NG-NCNT	0.90	0.71	-3.3	0.1 M KOH	1600	0.05	6
TTF-700-96	0.83	0.74	-4.6	0.1 M KOH	1600	-	7
NPCN	0.90	0.81	-5.0	0.1 M KOH	1600	0.71	8
C-PEOPAN-11-1000	0.88	-	-3.7	0.1 M KOH	1600	-	9

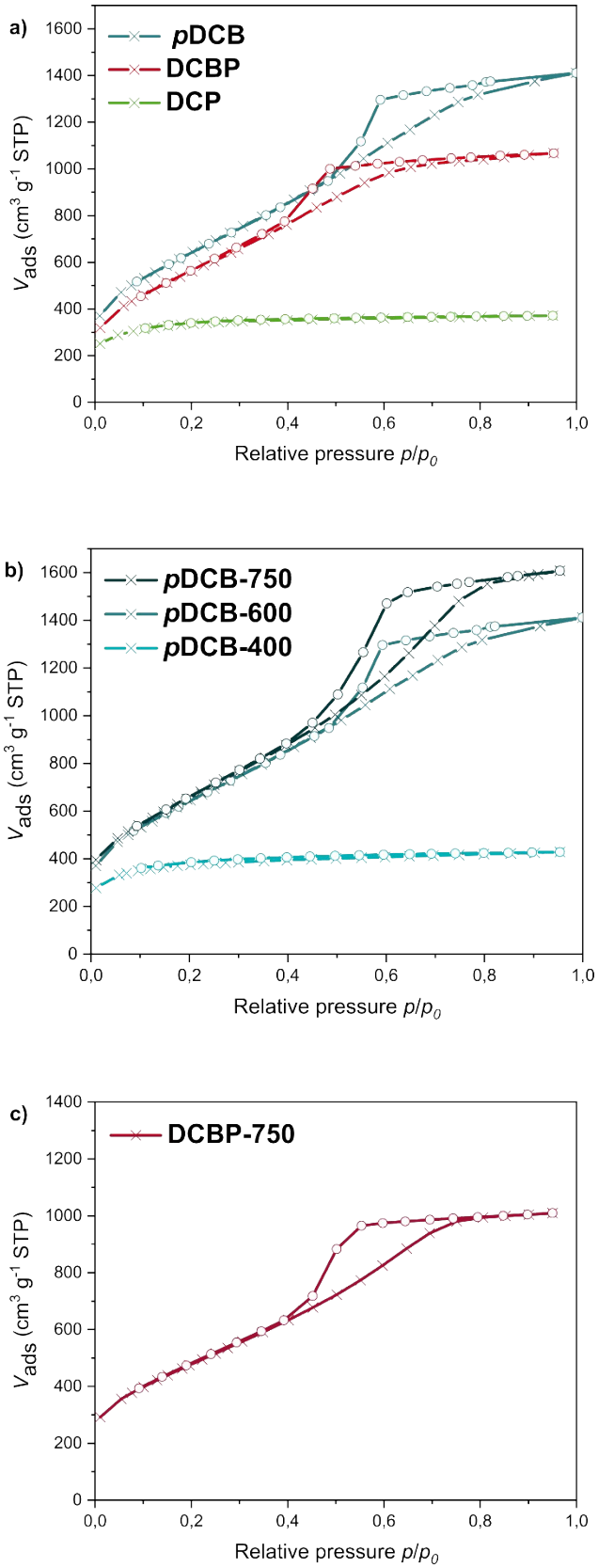

Figure S1. *Nitrogen physisorption isotherms of* ***(a)*** *the 3M-CTFs,* ***(b)*** *the 3T-CTFs and* ***(c)*** *CTF DCBP-750.*

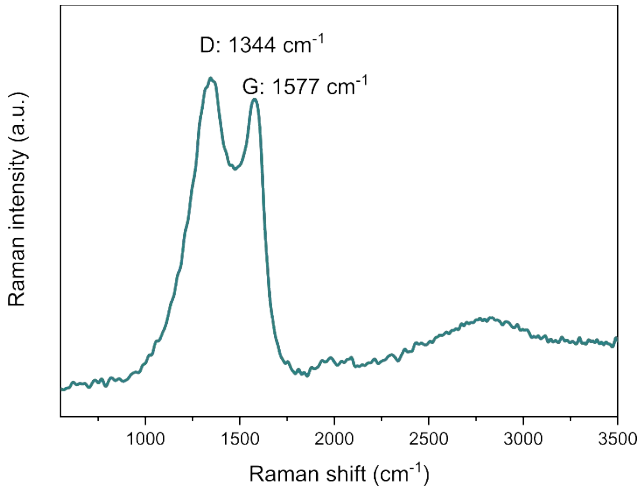

Figure S2. *Full Raman Spectrum of 3M-CTF pDCB. D and G bands and their corresponding Raman shifts are also shown in the figure.*

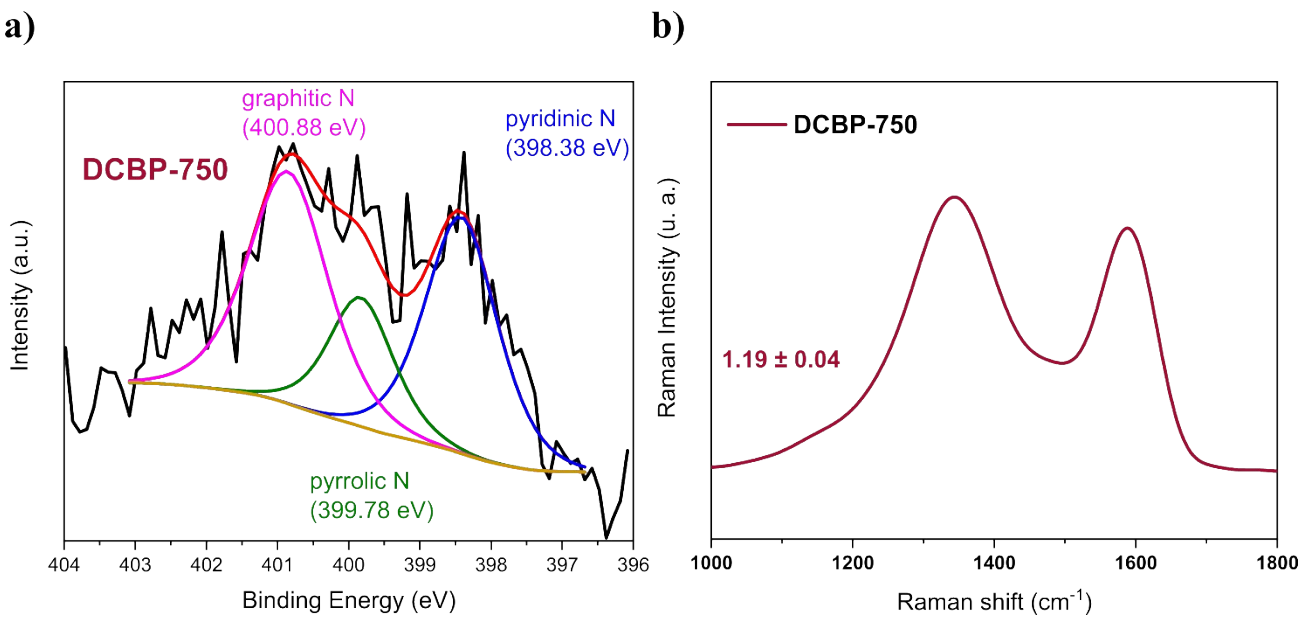

Figure S3. (a) *XPS N 1s deconvolution result of DCBP-750.* ***(b)*** *Raman Spectrum of DCBP-750. D (1344 cm^{-1}) and G (1577 cm^{-1}) bands and I_D/I_G value (1.19 ± 0.04).*

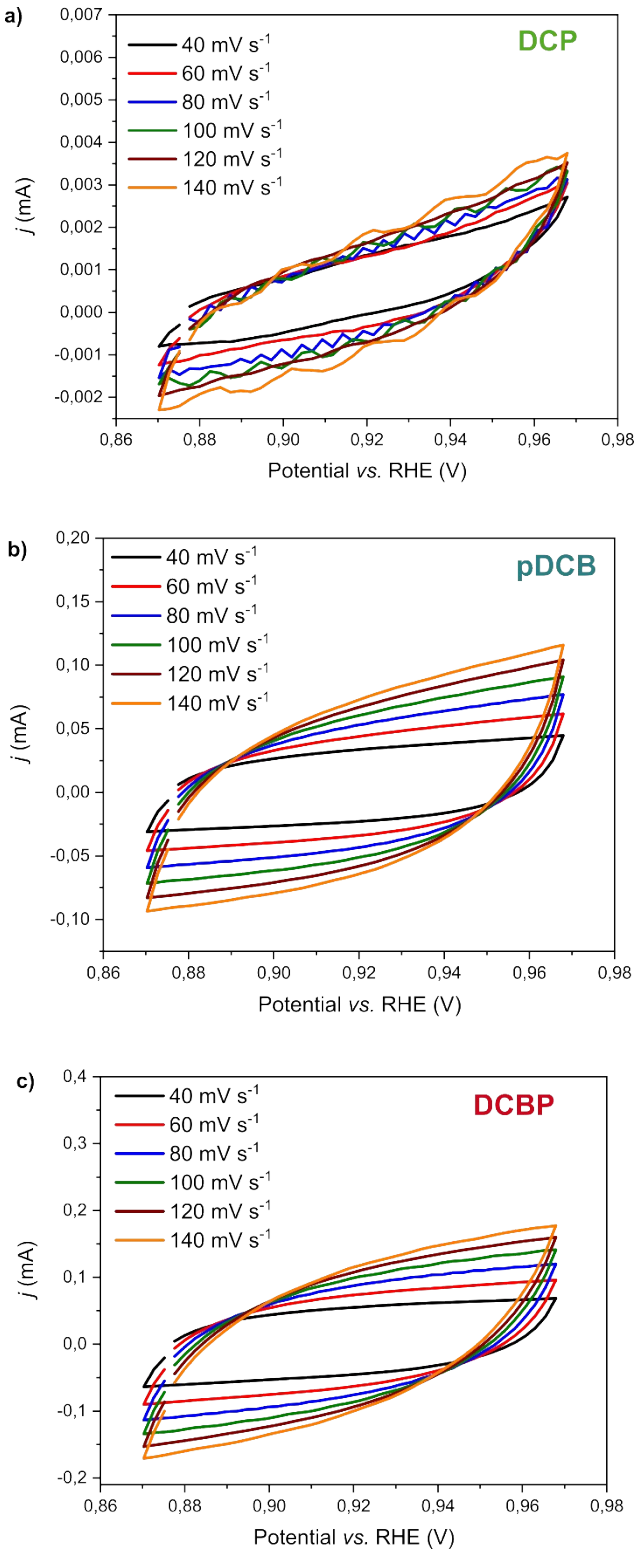

Figure S4. *Scan rate-dependent CV scans in non-Faradaic range for 3M-CTFs* ***(a)*** *DCP,* ***(b)*** *pDCB and* ***(c)*** *DCBP in 0.1 M KOH at 2500 rpm. The double layer capacitance slopes were obtained by plotting* Δi_a-i_c *(at 0.91 V vs. RHE.) vs. 2V (in which scan rates were multiplied by 2).*

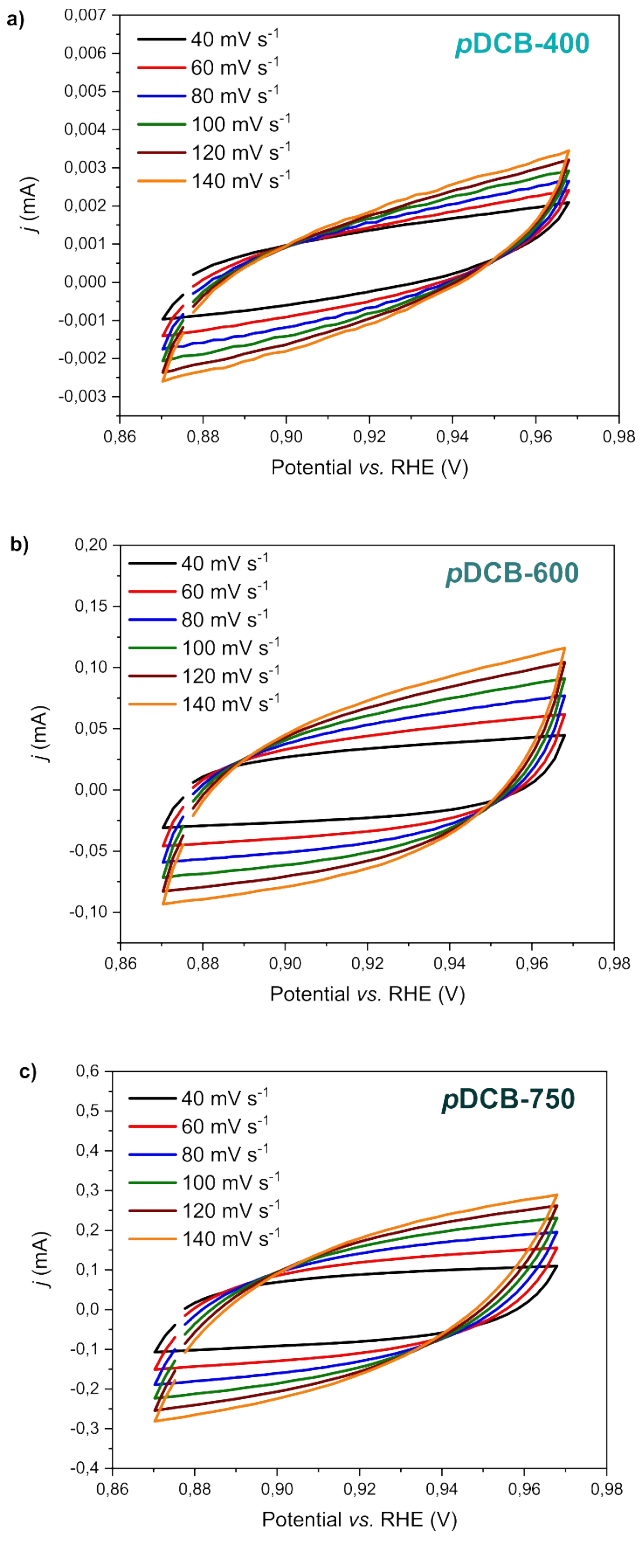

Figure S5. *Scan rate-dependent CV scans in non-Faradaic range for 3T-CTFs (**a**) pDCB-400, (**b**) pDCB-600 and (**c**) pDCB-750 in 0.1 M KOH at 2500 rpm. The double layer capacitance slopes were obtained by plotting* Δi_a-i_c *(at 0.91 V vs. RHE.) vs. 2V (in which scan rates were multiplied by 2).*

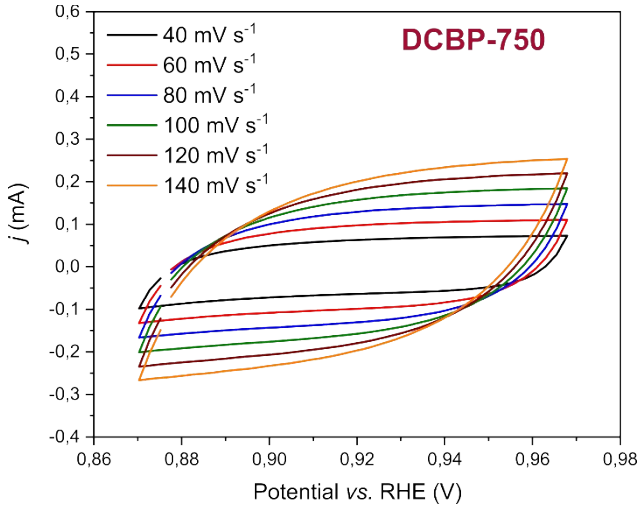

Figure S6. *Scan rate-dependent CV scans in non-Faradaic range for DCBP-750 in 0.1 M KOH at 2500 rpm. The double layer capacitance slopes were obtained by plotting* Δi_a-i_c *(at 0.91 V vs. RHE.) vs. 2V (in which scan rates were multiplied by 2).*

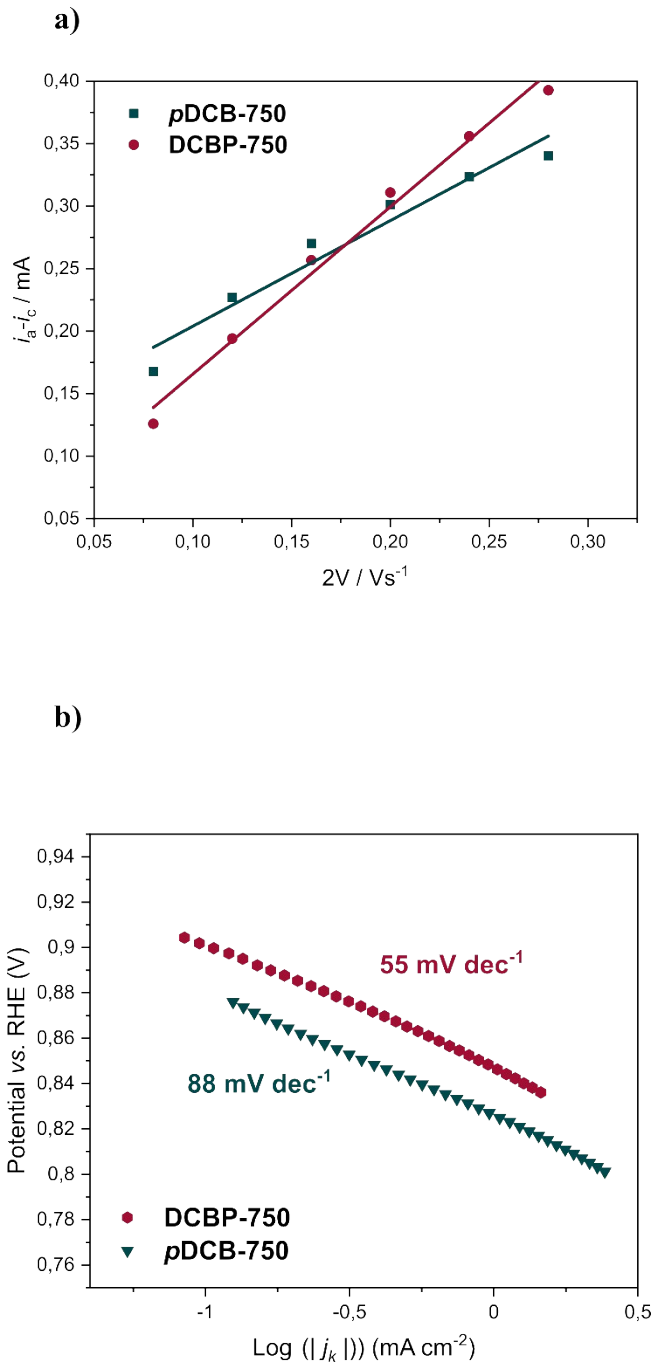

Figure S7. (a) *Plots for determination of the double layer capacitance based on scan rate-dependent cyclic voltammetry scans in non-Faradaic range (**Figure S5c** and **S6**, **Supporting information**, were used to obtain capacitance plots) and* ***b)*** *Tafel plots of CTFs DCBP-750 and pDCB-750 (data taken from the linear regions of the potential vs. logj_k at low current densities) recorded in 0.1 M KOH at a rotation rate of 2500 rpm.*

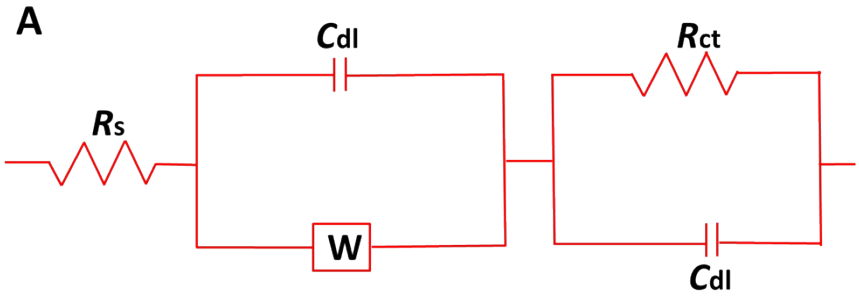

Figure S8A. *Suggested equivalent electrochemical circuits utilized to fit Nyquist and Bode plots for DCP, pDCB, pDCB-400, pDCB-600, pDCB-750 thin-film catalysts.* R_s *is the solution resistance, W is the Warburg impedance element, represents for mass-transfer process,* C_{dl} *is the double layer capacitance,* R_{ct} *is the charged transfer resistance controlled by the electrons transfer kinetics.*

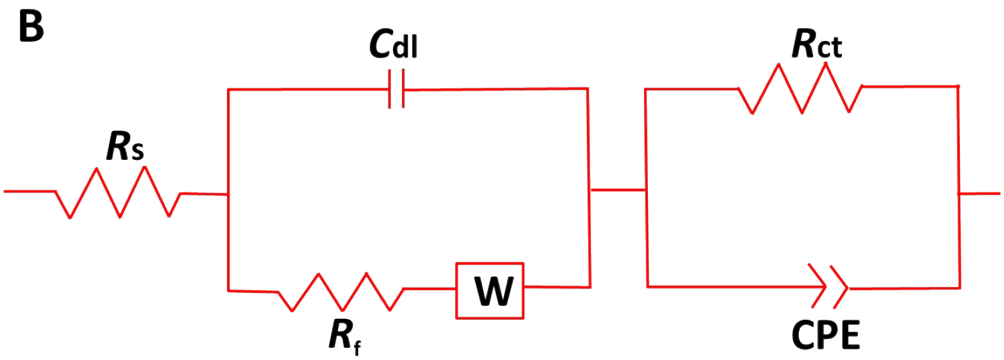

Figure S8B. *Suggested equivalent electrochemical circuits utilized to fit Nyquist and Bode plots for DCBP.* R_s *is the solution resistance,* R_f *is the thin-film catalyst resistance, W is the Warburg impedance element, represents for mass-transfer process,* C_{dl} *is the double layer capacitance, CPE is the constant phase element and* R_{ct} *is the charged transfer resistance, controlled by the electrons transfer kinetics.*

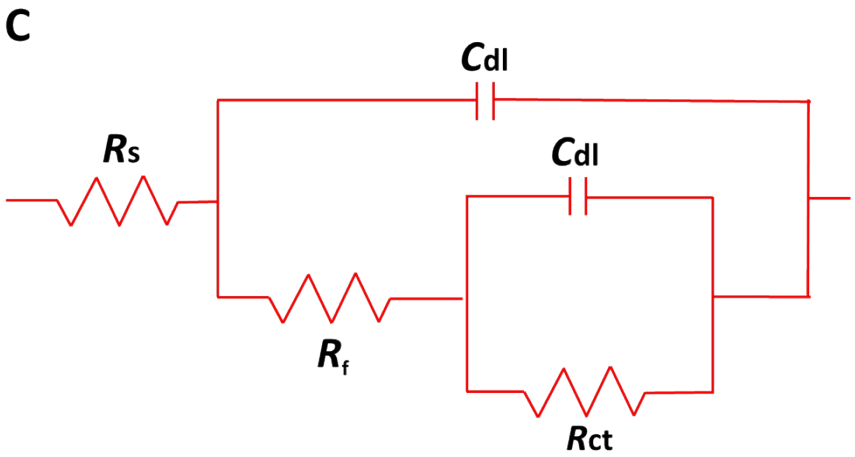

Figure S8C. *Suggested equivalent electrochemical circuits utilized to fit Nyquist and Bode plots for DCBP-750.* R_s *is the solution resistance,* R_f *is the thin-film catalyst resistance,* C_{dl} *is the double layer capacitance, and* R_{ct} *is the charged transfer resistance controlled by the electrons transfer kinetics.*

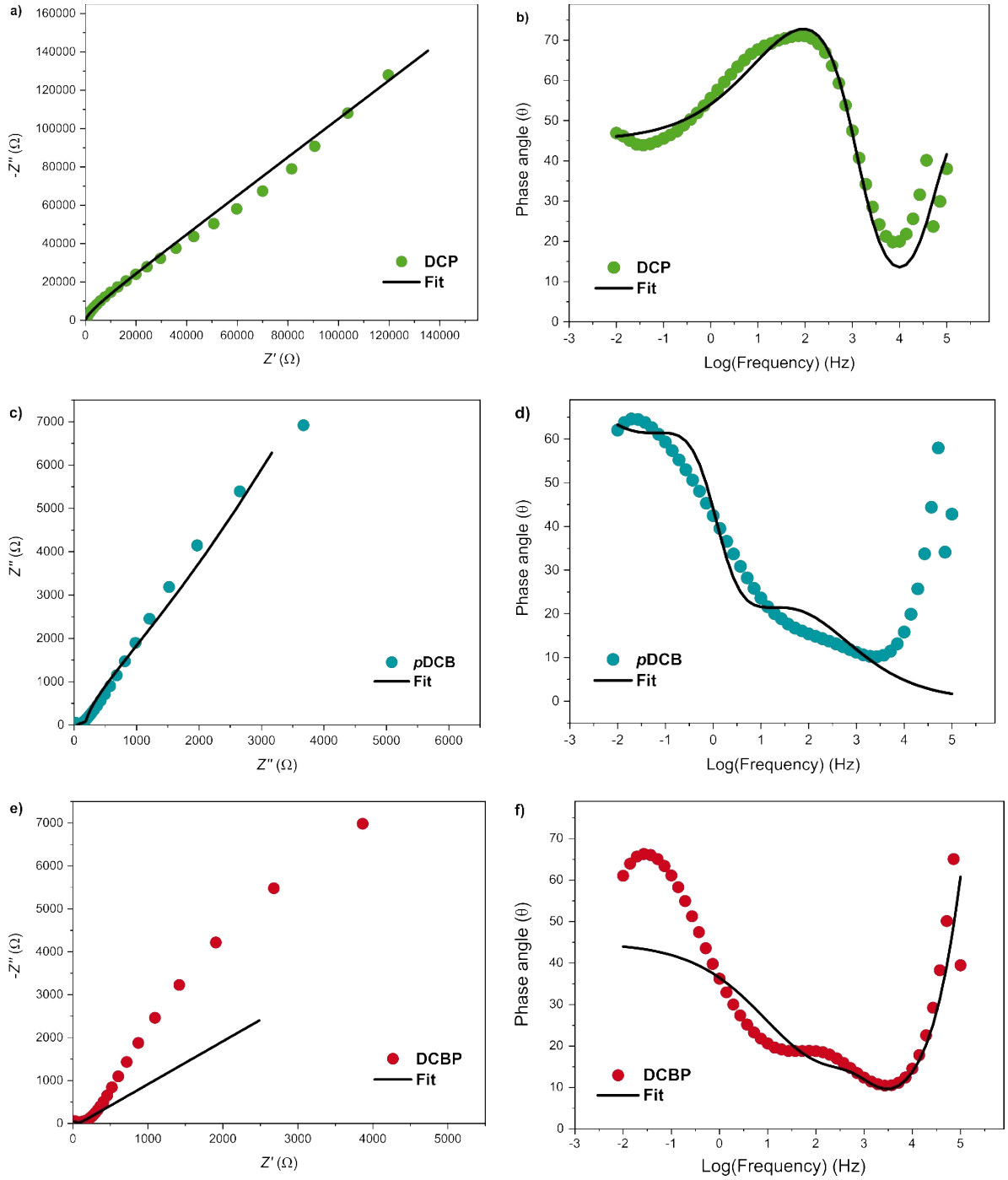

Figure S9. *Nyquist plots and corresponding Bode plots with resulting fitting curve for* ***3M-CTF DCP*** *(**a** and **b**),* ***pDCB*** *(**c** and **d**) and* ***DCBP*** *(**e** and **f**).*

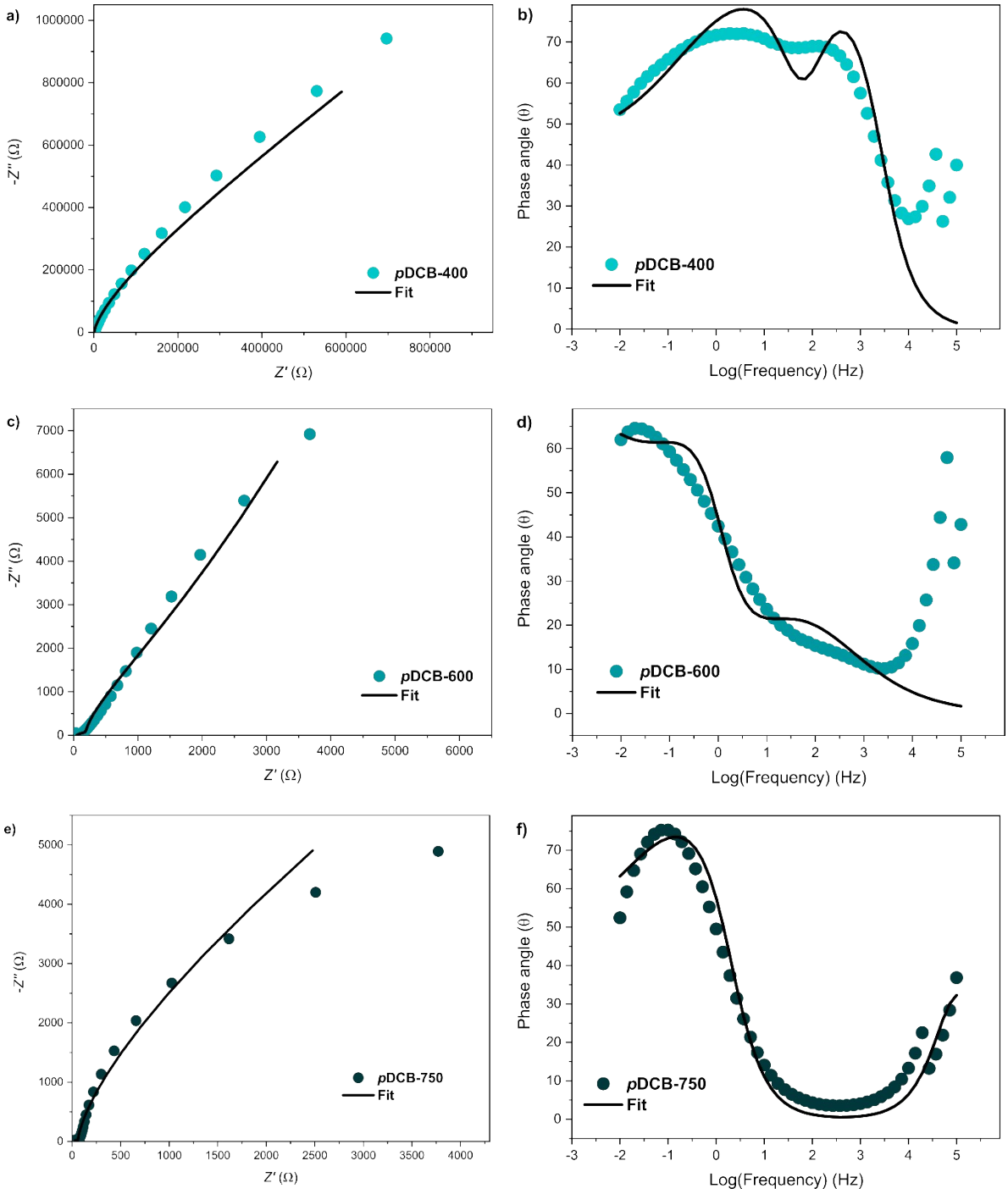

Figure S10. *Nyquist plots and corresponding Bode plots with resulting fitting curve for* ***3T-CTF pDCB-400*** *(**a** and **b**),* ***pDCB-600*** *(**c** and **d**) and* ***pDCB-750*** *(**e** and **f**).*

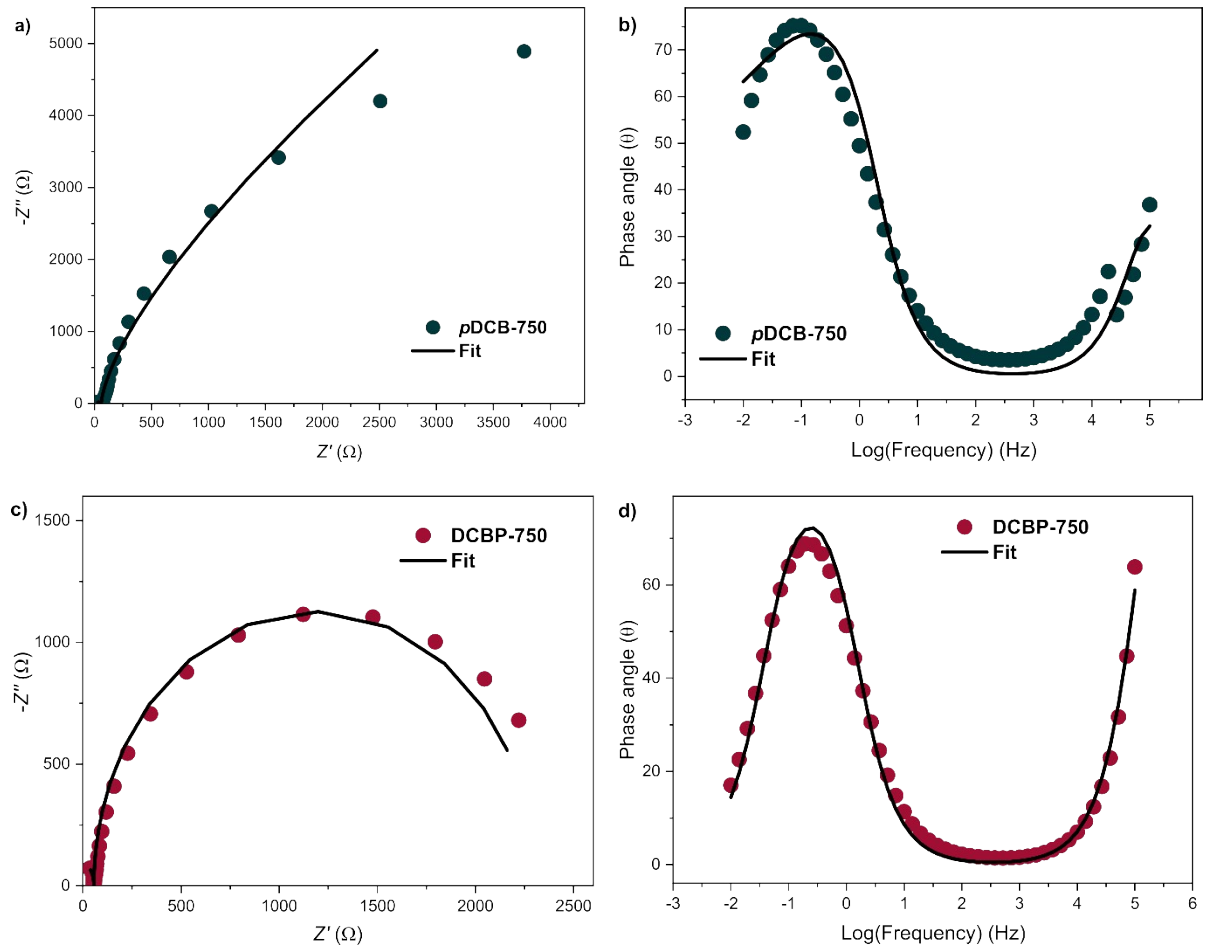

Figure S11. *Nyquist plots and corresponding Bode plots with resulting fitting curve for* ***pDCB-750*** *(**a** and **b**) and* ***DCBP-750*** *(**c** and **d**).*

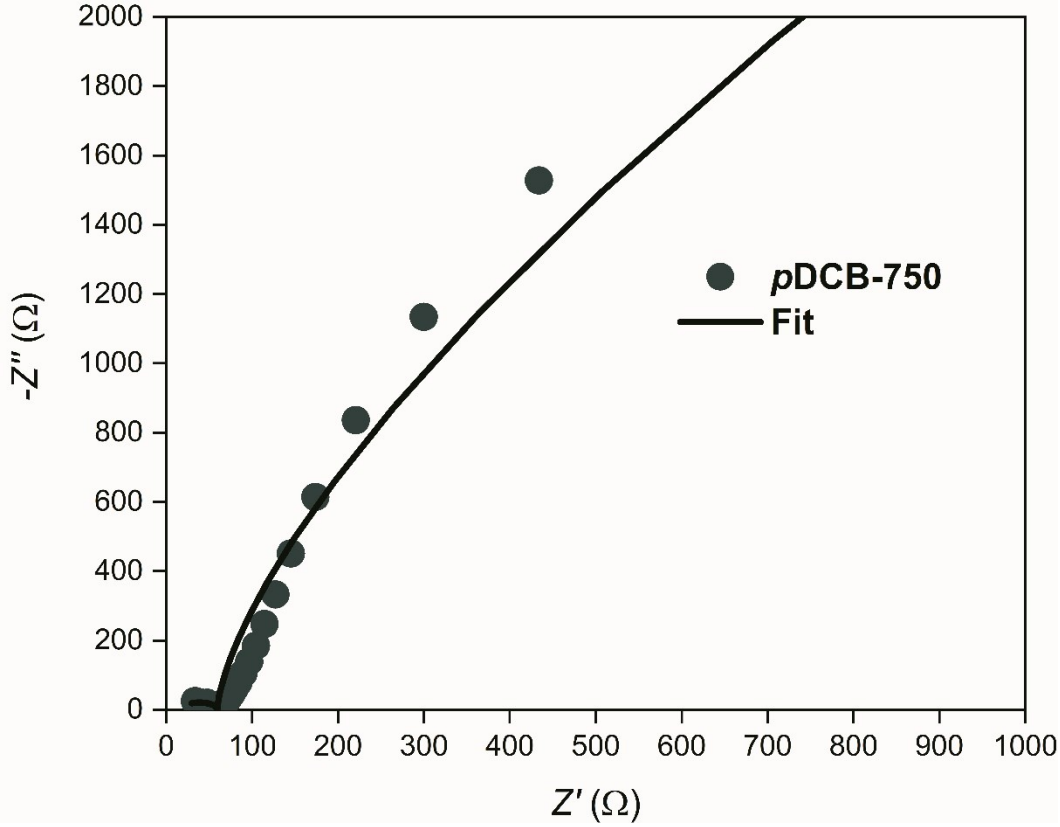

Figure S12. *Enlargement of the Nyquist plot for* ***pDCB-750.***

References

1 Y. Cao, Y. Zhu, X. Chen, B. S. Abraha, W. Peng, Y. Li, G. Zhang, F. Zhang and X. Fan, *Catal. Sci. Technol.*, 2019, **9**, 6606-6612.

2 L. Qu, Y. Liu, J.-B. Baek and L. Dai, ACS Nano, 2010, **4**, 1321-1326.

3 J. Masa, A. Zhao, W. Xia, M. Muhler and W. Schuhmann, *Electrochim. Acta*, 2014, **128**, 271-278.

4 X. Cui, S. Yang, X. Yan, J. Leng, S. Shuang, P. M. Ajayan and Z. Zhang, *Adv. Funct. Mater.*, 2016, **26**, 5708-5717.

5 W. Yu, S. Gu, Y. Fu, S. Xiong, C. Pan, Y. Liu and G. Yu, J Catal, 2018, 362, 1-9.

6 P. Chen, T.-Y. Xiao, Y.-H. Qian, S.-S. Li, S.-H. Yu, Adv. Mater. 2013, **25**, 3192-3196.

7 L. Hao, S. Zhang, R. Liu, J. Ning, G. Zhang and L. Zhi, *Adv. Mater.*, 2015, **27**, 3190-3195.

8 F. Pan, Z. Cao, Q. Zhao, H. Liang and J. Zhang, *Journal of Power Sources*, 2014, **272**, 8-15.

9 D. S. Yang, S. Chaudhari, K. P. Rajesh and J. S. Yu, *ChemCatChem*, 2014, **6**, 1236-1244.